PEOPLE'S DEMOCRATIC REPUBLIC OF ALGERIA

Ministry of Higher Education and Scientific Research

University of Amar Telidji - Laghouat

Faculty of Technology

Department of Electronics

MASTER THESIS

DOMAIN: Science & Technology

FIELD: Automation

SPECIALTY: Automation & Industrial Computing

Bentourki Marouane & **Lagmi Messaoud**

Theme

Design, Implementation and Advanced Control of a Push-Pull Power Converter

Jury members:

BELKHIRI Mohammed	Prof	President
HADJAISSA Aboubakeur	MCA	Examiner
BENMILOUD Mohammed	MCB	Supervisor
AMEUR Khaled	MCB	Co-Supervisor

2022 / 2023

Abstract

The purpose of this master project is to build a DC/DC power converter, known as push-pull power converter. The converter is widely used in photovoltaic systems which allows to increase the DC voltage by the mean of a set of switches, a transformer, rectifier and a filter.

To guarantee a good operation of the converter, a linear quadratic regulator (LQR) is proposed which ensures the stabilization of the output voltage around a given reference.

Simulation and experimental results show the effectiveness of the experimental setup and its control scheme under load and input voltage variations.

Keywords: Push-Pull Converter,LQR, Dspace ds1103, solar inverter.

ملخص

الغرض من هذا المشروع الرئيسي هو بناء محول طاقة مستمر–مستمر،المعروف باسم محول طاقة الدفع والسحب.يستخدم المحول على نطاق واسع في الأنظمة الكهروضوئية مما يسمح بزيادة جهد التيار المستمر عن طريق مجموعة من المفاتيح،ومحول، ومقوم ومرشح .

يضمن استقرار جهد الخرج (LQR) لضمان التشغيل الجيد للمحول، يُقترح وجود منظم تربيعي خطي حول مرجع معين.

أظهرت نتائج المحاكاة والتجريب فعالية الإعداد التجريبي ومخطط التحكم الخاص به تحت تغيرات الحمل وجهد الدخل.

الكلمات المفتاحية :محول الدفع والسحب ، المنظم التربيعي الخطي ، (DSPACE ds1103)، العاكس للطاقة الشمسية.

Acknowledgements

We would like to express our special appreciation and thanks to our esteemed supervisors Mr. BENMILOUD Mohammed and Mr. AMEUR Khaled. We would like to thank them for their unwavering support and encouragement throughout our research journey. Their guidance paved the way for the successful completion of our master's thesis. We would also like to express our sincere thanks to the committee members, Prof. BELKHEIRI Mohammed and Dr. HADJAISSA Aboubakeur for their invaluable contributions and feedback.

We are particularly grateful to our families; words cannot adequately convey the depth of our gratitude for the sacrifices they have made and the unwavering support and prayers that sustained us. We would also like to thank all of our friends who supported us in preparing this project, and incented us to strive towards our goal.

Special thanks to LACoSERE and LTSS laboratory members. Their support and benefic discussions make the way to accomplish this work easy.

BENTOURKI Marouane & LAGMI Messaoud
Laghouat University
September 2023

Contents

List of Figures

General Introduction

DC-DC converters play a crucial role in our daily lives, serving as essential components in numerous electronic devices and systems. Their ability to efficiently transform one voltage level to another enables a smooth operation of a wide range of applications, from portable phones to renewable energy systems.

In the realm of photovoltaic systems, where the conversion of DC power to AC power is fundamental, the use of isolated DC-DC converters has gained prominence due to their reliability and safety features.

This master thesis is a part of a research project conducted within the ACS Team of the LACoSERE laboratory, focusing on the development and advanced control of static converters for photovoltaic systems.

The core of this master's thesis is dedicated to the implementation and control of a push-pull power converter, a key component widely used in the DC-to-DC stage of solar inverters. This has been successfully attained and comprehensively outlined within four chapters:

- In **Chapter One**, we presented an overview of DC-DC power converters, highlighting the distinction between isolated and non-isolated topologies. Furthermore, we introduced an algorithm designed to facilitate the selection of the most suitable power converter topology, based on power, voltage, and current requirements.

- **Chapter Two** comprehensively explores the operational principles of the push-pull converter, offering a detailed examination of its mathematical foundations. In addition to that, we presented a linear quadratic regulator for the push pull converter where the controller objective is to regulate its output voltage.

- In **Chapter Three**, we presented various components of the experimental setup, encompassing the converter itself, isolation as well as the dSPACE and DSP control boards, and measurement devices.

- **Chapter Four** presents the main results obtained from simulations and experimental setup of

the push pull converter. We initially examine its performance in an open-loop configuration, followed by an assessment of the effectiveness of the linear quadratic regulator in controlling the push-pull converter

Chapter 1

An Overview of Isolated DC-DC Converters

Contents

1.1 Introduction

This chapter provides an introduction to isolated DC-DC power converters, focusing on the following key aspects: a comparison between isolated and non-isolated power converters, the advantages of isolation, various types of isolated converters and how to choose the right one for your application. Furthermore, this chapter offers a comprehensive exploration of the selected topology for this project.

1.2 What is a DC/DC power converters

DC-DC converters, also known as voltage converters or power converters, are electronic circuits or devices used to convert a DC input voltage to a different DC output voltage level.

They are widely used in various applications where there is a need to step up or step down the voltage level, such as power supplies, battery-powered devices, renewable energy systems, automotive electronics, and more. The primary function of a DC-DC converter is to efficiently transfer power from the input source to the output load while maintaining the desired output voltage level. These converters can perform voltage step-up (boost), voltage step-down (buck), or both (buck-boost) conversions depending on the specific design.

In this type of Converters, there is no isolation between the input and the output, and for this reason their use is limited (applications that do not need insulation). Next, we will give examples of converters about them.[1].

1.2.1 Buck converter

Buck converters are one of the simplest, cheapest and most common topologies (see Fig.1.1). While this topology is not suited for applications where isolation is required, it is ideal as a DC to DC converter used to step-down voltages. Not only you can achieve high efficiency levels, but also high power levels using a buck converter, especially with poly-phase topologies. The down side of a buck converter is that the input current is always discontinuous, resulting in higher EMI.[2].

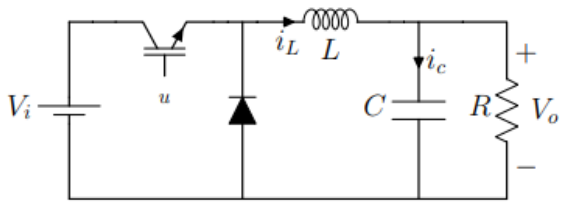

Figure 1.1: Buck converter circuit diagram.

1.2.2 Boost converter

The boost topology, like the buck topology, is a non-isolated power converter. Unlike the buck topology, the boost steps up the voltage rather than stepping it down. Because the boost topology draws current in a continuous, even manner when operating in continuous conduction mode, it is an ideal choice for Power Factor Correction circuits. Fig.1.2 shows the topology of a typical DC-DC boost converter associated with a resistive load[2].

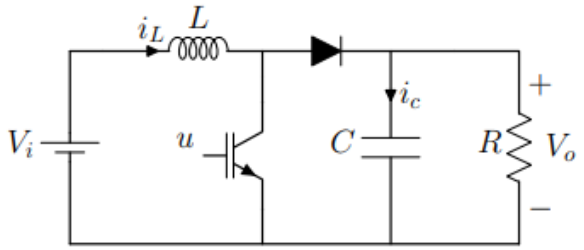

Figure 1.2: Boost converter circuit diagram.

1.2.3 Buck-Boost converter

The buck-boost topology can either step the voltage up or down. Fig. 1.3illustrates a circuit diagram of a Buck-Boost converter. This topology is particularly useful in battery powered applications, where the input voltage varies over time but has the disadvantage of inverting the output voltage. Another disadvantage of the buck-boost topology is that the switch does not have a ground, which complicates the drive circuit.[2].

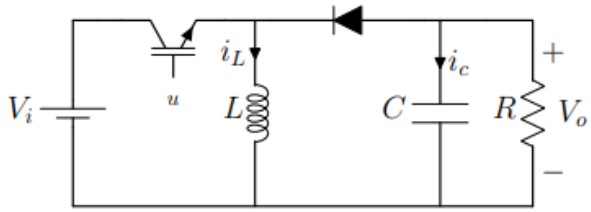

Figure 1.3: Buck-Boost converter circuit diagram.

1.3 Isolated Dc/DC power converter

In a typical DC-DC converter, a single regulator circuit enables direct current flow from input to output, offering advantages such as reduced complexity, compact size, and cost-effectiveness. However, certain applications necessitate *galvanic isolation*, hereafter referred to as "isolation".[3]

1.3.1 What Isolation means?

Isolation (galvanic isolation) means the absence of a direct conduction pathway between two parts of a circuit. This isolation consistently acts as a barrier between the input and output stages, serving vital roles in ensuring circuit functionality, safety, or a combination of both.

In an isolated converter, the input and output stages have separate grounds, while in a nonisolated

converter, they share a common ground, allowing current to flow directly between the two sides. It is typically achieved by integrating a transformer into the circuit, facilitating power transfer through electromagnetic energy (see Fig.1.4). While this approach does introduce some efficiency losses, careful transformer design can help minimize these losses.

Figure 1.4: Example of a set of transformers used for galvanic isolation in DC-DC converters.

1.3.2 Benefits Of isolation

One of the most significant benefits of isolation lies in ensuring safety compliance. The isolation barrier acts as a safeguard, effectively blocking the transmission of hazardous mains voltages to the output, thereby preventing potential contact. This aspect holds particular importance in applications like the medical field, where direct patient circuit connections are involved.

In numerous applications, noise interference poses a significant concern. Isolated power supplies, thanks to their absence of shared grounds, offer a solution by effectively breaking ground loops within the circuit.[4].

1.3.3 Main types of Isolated DC-DC converters

FlyBack Converter

Fig. 1.5 shows the flyback converter circuit diagram which is a simple and versatile DC/DC converter that is well-suited for a wide range of applications. It is typically used for low- to medium-power applications, such as TVs, computers, power supplies for industrial and medical equipment, and solar power inverters. This returns to a number of advantages that this structure offers, such as:

- **Simplicity:** It requires only a few components, and it is relatively easy to design and build.
- **Versatility:** The flyback converter can be used for a wide range of input and output voltage ranges. It can also be used to generate multiple outputs.

- **Cost:** Flyback converters are typically less expensive than other isolated DC/DC converter topologies.

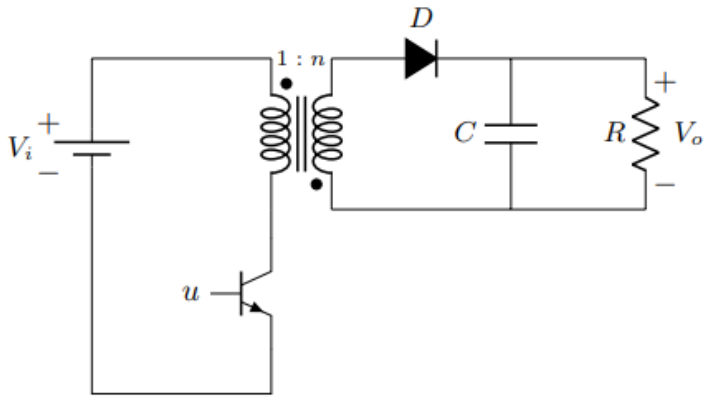

Figure 1.5: : Circuit diagram of a flyBack converter.

It should be noted that the flyback converter also has some disadvantages, including *Lower efficiency at high power levels*. This is because of the energy losses associated with the switching transistor and the transformer. In addition, the flyback converter has relatively *high ripple current* at the output.

Forward converter

The forward converter is really just a transformer isolated buck converter. Like the flyback topology, the forward converter is best suited for lower power applications. While effiiency is comparable to the flyback, it does have the disadvantage of having an extra inductor on the output and is not well suited for high voltage outputs. The forward converter does have the advantage over the flyback converter when high output currents are required. Since the output current is non-pulsating, it is well suited for applications where the current is in excess of 15A. [5]

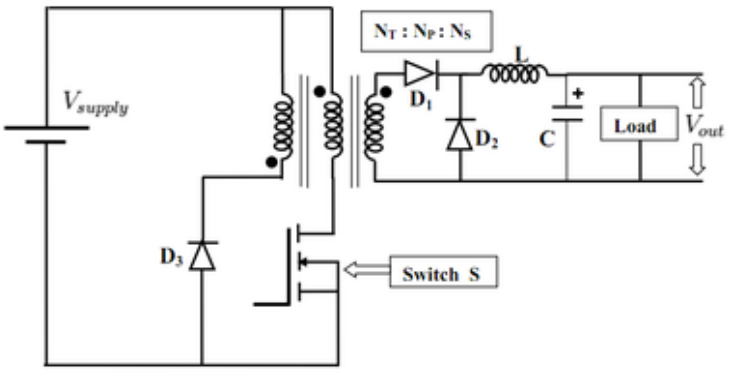

Figure 1.6: Forward Converter

Full-bridge converter

The transformer topology for both the Half Bridge and Full Bridge converter is the same, except that for a given DC link voltage of the Half Bridge transformer sees half the applied voltage as compared with that of the Full Bridge transformer. The current flows in opposite directions during alternate half cycles. So flux in the core swings from negative to positive, utilizing even the negative portion of the hysteresis loop, thereby, reducing the chances of core saturation. Therefore, the core can be operated at greater 50 value here. The largest power is transferred when the duty cycle is less than 50 Diagonal pairs of transistors (Q1-Q4 or Q2-Q3) conduct alternately, thus, achieving current reversal in the transformer primary. Output voltage equals:

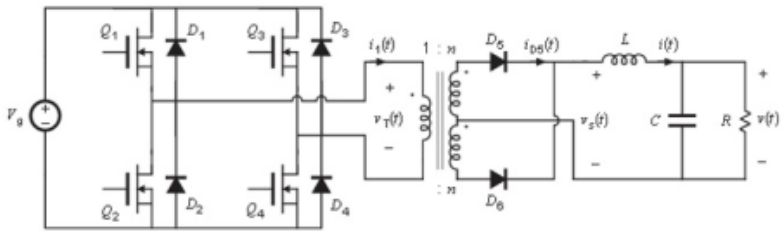

Figure 1.7: Full-bridge converter

Push-pull converter

The push-pull converter topology is essentially a forward converter with two primary winding used to create a dual drive winding. This utilizes the core of the transformer much more efficiently than the flyback or the forward converters. On the other hand, only half the copper is being used at a time, thereby increasing the copper losses significantly in a similar sized transformer. For similar power levels, the push-pull converter will have smaller filters compared to the forward converter.

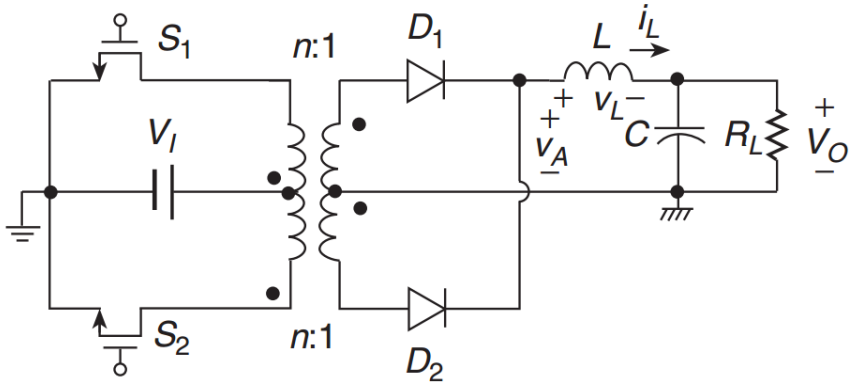

Figure 1.8: Push-pull converter

1.3.4 How to choose the right DC-DC converter?

Choosing the right DC-DC converter depends on the application requirements which mainly can be limited to current, voltage and power levels. Fig.1.9 shows a simple diagram that can be useful for which converter topology that can we use.

1.4 Project Description

This master's project is an integral component of the ongoing research conducted within the LA-CoSERE laboratory, with a primary focus on the advancement of power conversion structures and the implementation of advanced control strategies tailored specifically for solar inverters. Within the

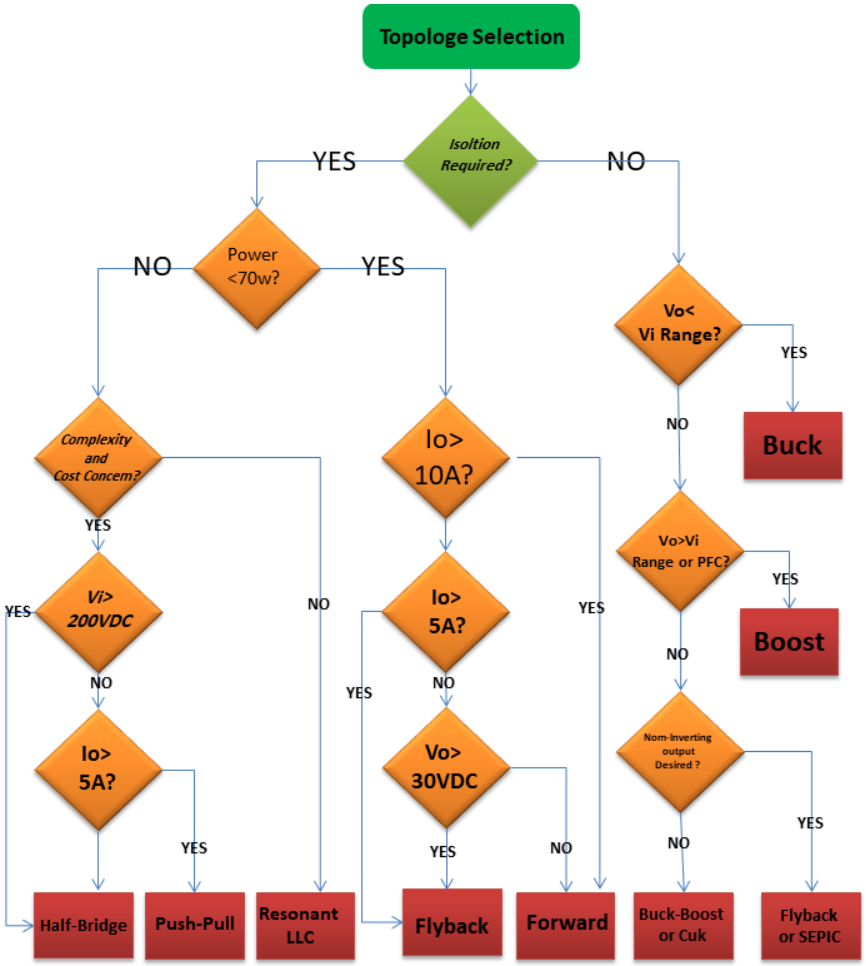

Figure 1.9: : Topology Selection

realm of commercial solar inverters, a fundamental aspect involves the conversion of direct current

(DC) into alternating current (AC) through two distinct stages. The initial phase, known as the DC to DC stage, is predominantly constructed upon the *push-pull converter topology.*

Fig. 1.10 illustrates some solar inverters studied at LACoSERE laboratoy which incorporate a push-pull converter in the DC-DC stage. This fact has motivated the control team to exploit this topic from modelling to control design and implementation. In order to reach this objective in a structured way, the following tasks are defined for this project. These points will be addressed in next chapters.

- **Task 1:** Converter modeling.
- **Task 2:** Controller design and validation through simulations.
- **Task 3:** Converter implementation and experimental validation

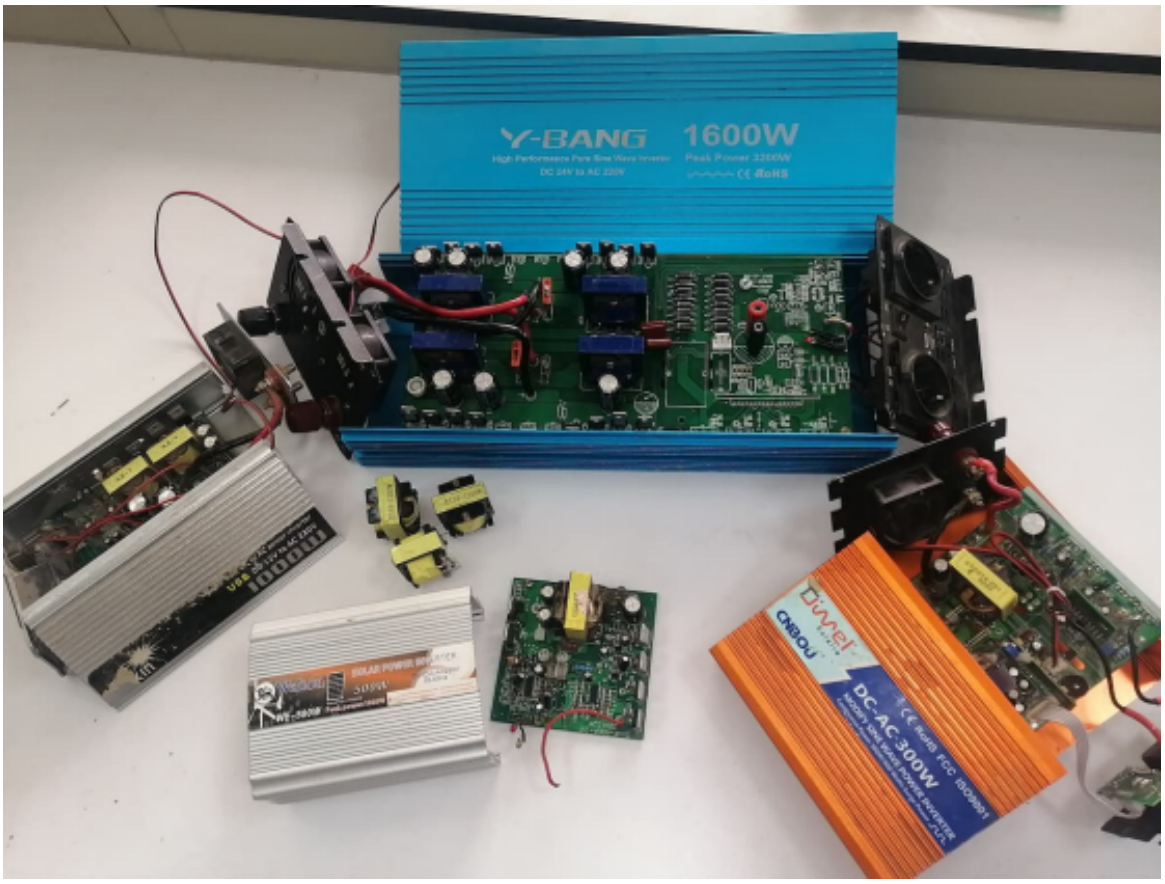

Figure 1.10: Commercial Solar Inverters incorporating push-pull converter.

1.5 Conclusion

In this chapter, we highlighted the difference between isolated and non-isolated converters. Then, we justified the topology choice (push-pull converter) in this master thesis. The next chapter will be devoted to modelling and control design for the converter in question.

Chapter 2

Modelling & Control of Push-Pull Converter

Contents

2.1 Introduction

The push-pull converter is a popular type of DC-DC converter that is widely used in various power electronic applications. It offers advantages such as high efficiency, compact size, and bidirectional operation. To ensure proper operation and control of the push-pull converter, it is essential to develop an accurate mathematical model and design appropriate control strategies.

2.2 Description of Push Pull Converter

Figure 2.1 shows the circuit diagram of a push-pull DC/DC power converter supplying a resistive load. The main components of a push-pull converter are [6]:

- **Two active switches:** These are typically MOSFETs or IGBTs. The switches are turned ON and OFF alternately to control the flow of current through the transformer.
- **A transformer:** The transformer is used to transfer energy from the primary to the secondary side of the converter. It also provides electrical isolation between the input and output circuits.
- **A diode bridge:** The diode bridge is used to rectify the output voltage from the transformer.
- **The filter LC:**The filter of a push-pull converter is used to smooth out the output voltage and reduce ripple.

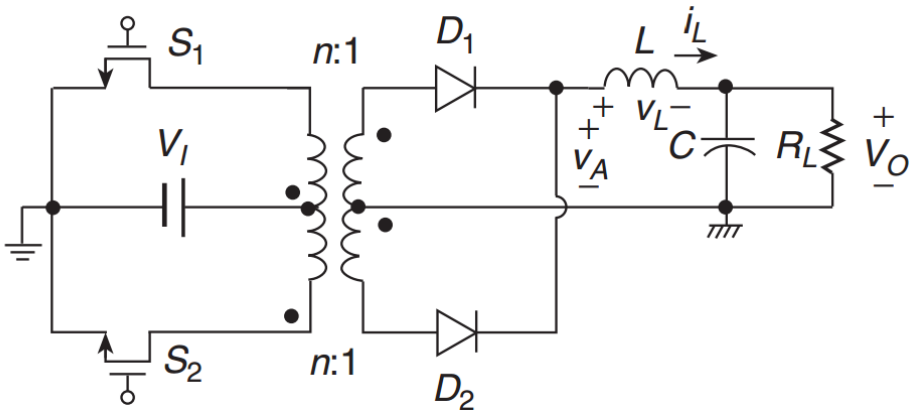

Figure 2.1: Push-pull converter topology schematic

Maximum number of possible modes is defined by the states of the switching devices (ON, OFF). It should be noted that the case where S1 and S2 are ON at the same time yields to a short circuit. Taking this into account, the total number of feasible states is *three*. Table 2.1 reports different operation modes of a push pull converter (excluding the dangerous mode).

STATES	S1	S2	D1	D2
Mode 1	ON	OFF	ON	OFF
Mode 2	OFF	OFF	OFF	OFF
Mode 3	OFF	ON	OFF	ON

Table 2.1: Operation modes of a Push-pull converter.

2.2.1 Operation of Push Pull Converter

The analysis of the push-pull converter is based on the following assumptions:

- The power MOSFETs and the diodes are ideal switches.
- The transistor and diode capacitances and the lead inductances are zero.
- The converter is operated in steady state.

Fig. 2.2 shows the converter waveforms over one switching period (period of PWM). Next, we will thoroughly explore each operation mode.

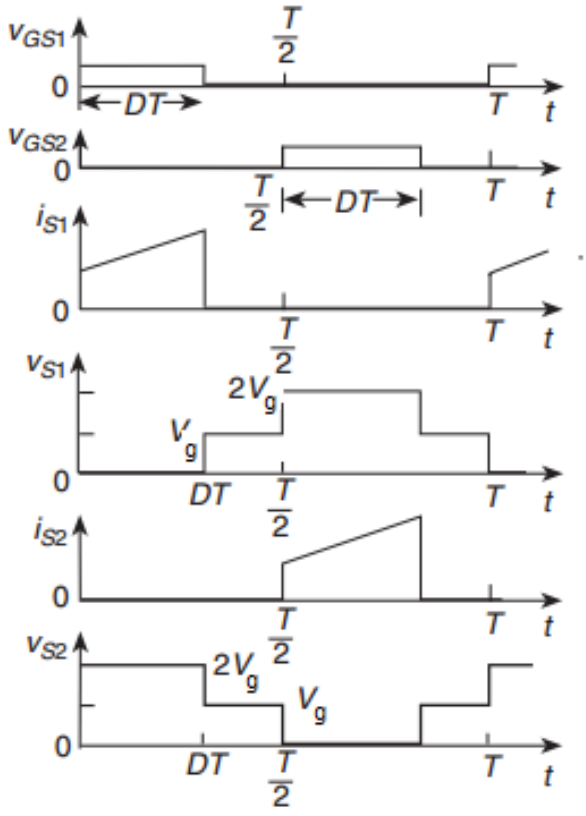

Figure 2.2: Waveforms of the push–pull converter

Mode 1:when S1 is ON and S2 is OFF

During the time interval $0 < t \leq DT$, the switch S1 and diode D1 are ON and the switch S2 and diode D2 are OFF. An ideal equivalent circuit for this time interval is shown in Figure 2.3. Equations for this state:

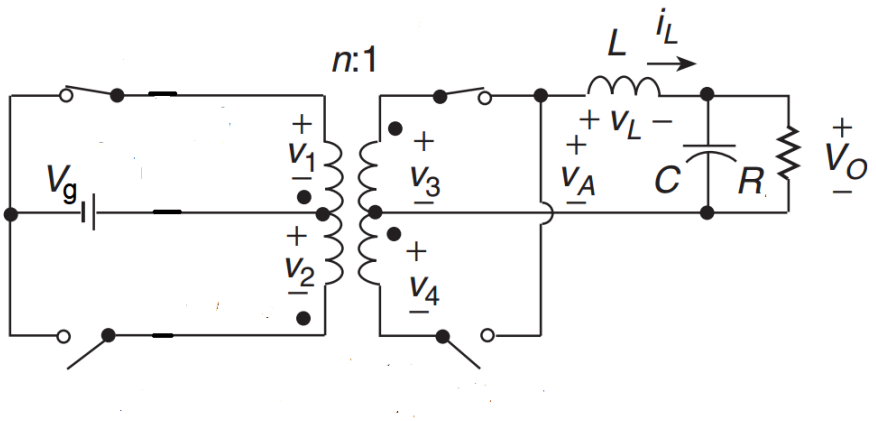

Figure 2.3: Mode 1 circuit diagram.

$$V_1 = -V_g \tag{2.1}$$

The voltage across the lower primary :

$$V_2 = V_1 = -V_g \tag{2.2}$$

The voltage across the upper secondary is:

$$V_3 = -V_1/n = V_g/n \tag{2.3}$$

The voltage across the lower secondary is:

$$V_4 = V_3 = V_g/n \tag{2.4}$$

the voltage across the switch S1 and switch S2

$$\begin{gathered} V i_L = 0 \\ V S_2 = (V_g + V_2) = (V_g + V_g) = 2V_g \end{gathered} \tag{2.5}$$

The voltage across the diode D2:

$$\begin{gathered} V D_2 = -(V_3 + V_4) = -(V_g/n + V_g/n) \\ V D_2 = -2V_g/n \end{gathered} \tag{2.6}$$

The voltage at the input to the low-pass filter is :

$$V_A = V_3 = \frac{V_g}{n} \tag{2.7}$$

The voltage across the inductor L is:

$$V_L = L\frac{di_L}{dt} = \frac{V_g}{n} - V_o \tag{2.8}$$

The currents in inductor L:

$$i_L = i_3 = i_{D_1} \tag{2.9}$$

The currents of capacitor:

$$\begin{aligned} i_c &= i_L - i_o \\ i_c &= C\tfrac{dV_o}{dt} \\ io &= \tfrac{1}{R}V_c \\ C\tfrac{dV_c}{dt} &= i_L - \tfrac{V_o}{R} \end{aligned} \tag{2.10}$$

The dynamic model of this mode is:

$$V_L = L\frac{di_L}{dt} = \frac{V_g}{n} - V_o \tag{2.11}$$

$$C\frac{dV_c}{dt} = i_L - \frac{V_o}{R} \tag{2.12}$$

$$V_A = V_g/n \tag{2.13}$$

The dynamic model of this mode is $\dot{x} = A_1 x + B_1$:

Mode 1 dynamic model:

$$\underbrace{\frac{d}{dt}\begin{bmatrix} i_L \\ Vo \end{bmatrix}}_{\dot{x}} = \underbrace{\begin{bmatrix} 0 & -\frac{1}{L} \\ \frac{1}{C} & -\frac{1}{RC} \end{bmatrix}}_{A_1} \underbrace{\begin{bmatrix} i_L \\ Vo \end{bmatrix}}_{x} + \underbrace{\begin{bmatrix} \frac{Vg}{nL} \\ 0 \end{bmatrix}}_{B_1} \tag{2.14}$$

Mode 2:when S1 is OFF and S2 is OFF

Figure 2.4 shows an equivalent circuit of the push-pull converter for the time interval $DT < t \leq \frac{T}{2}$, during which both switches are OFF and both diodes are ON. The currents through the secondaries are equal in magnitude and flow in opposite directions, resulting in zero magnetic flux in the core. Therefore, the voltages across the transformer windings are:

$$V_1 = V_2 = V_3 = V_4 = 0 \tag{2.15}$$

The voltages across the switches:

$$Vs_1 = Vs_2 = V_g \tag{2.16}$$

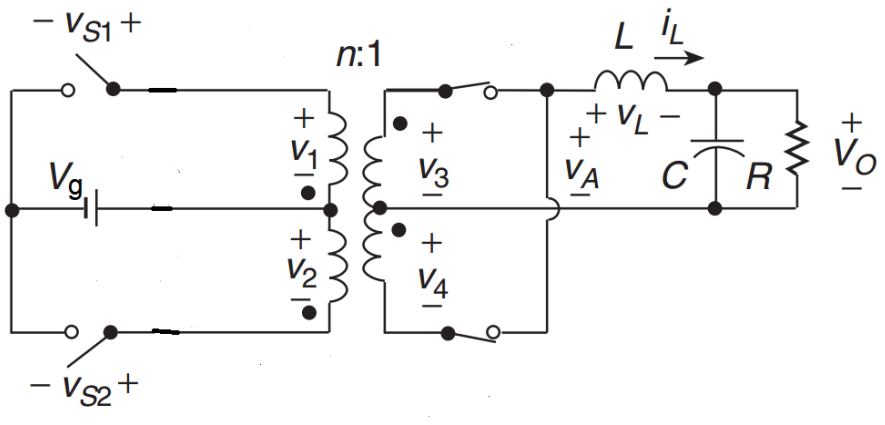

Figure 2.4: Mode 2 circuit diagram.

The voltage across the inductor L is:

$$V_L = L\frac{di_L}{dt} = -V_o \tag{2.17}$$

The voltage at the input to the low-pass filter is :

$$V_A = V_3 = 0 \tag{2.18}$$

The dynamic model of this mode is:

$$V_L = L\frac{di_L}{dt} = \frac{V_g}{n} - V_o \tag{2.19}$$

$$C\frac{dV_c}{dt} = i_L - \frac{V_o}{R} \tag{2.20}$$

$$V_A = 0 \tag{2.21}$$

The dynamic model of this mode is $\dot{x} = A_2x + B_2$:

Mode 2 dynamic model:

$$\underbrace{\frac{d}{dt}\begin{bmatrix} i_L \\ Vo \end{bmatrix}}_{\dot{x}} = \underbrace{\begin{bmatrix} 0 & -\frac{1}{L} \\ \frac{1}{C} & -\frac{1}{RC} \end{bmatrix}}_{A_2}\underbrace{\begin{bmatrix} i_L \\ Vo \end{bmatrix}}_{x} + \underbrace{\begin{bmatrix} 0 \\ 0 \end{bmatrix}}_{B_2} \tag{2.22}$$

Mode 3:when S1 is OFF and S2 is ON

Figure 2.5 shows an equivalent circuit of the converter for the time interval $\frac{T}{2} < t \leq \frac{T}{2} + DT$ during which the switch S1 and diode D1 are and the switch S2 and diode.The **mathematical equations are the same as the equations for Mode 1,** they differ in the transformer equations shown below

$$\begin{aligned} V_2 &= V_g \\ V_1 &= V_2 \\ V_3 &= -\frac{V_1}{n} = -\frac{V_g}{n} \\ V_4 &= V_3 = -\frac{V_g}{n} \end{aligned} \tag{2.23}$$

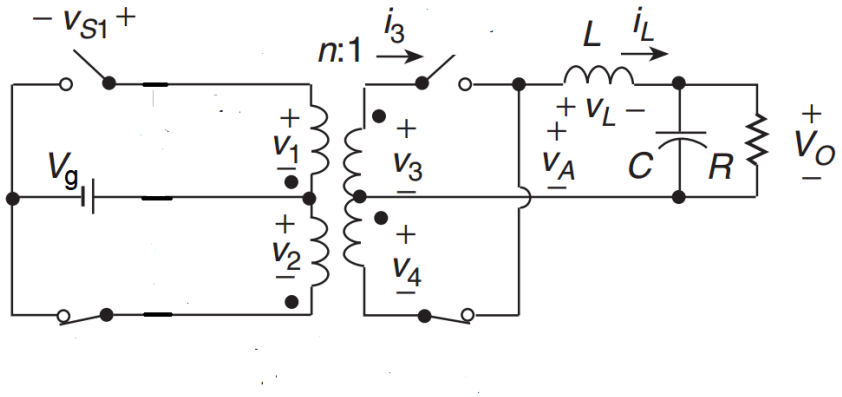

Figure 2.5: Mode 3 circuit diagram.

2.3 Average model of a push pull converter

In previous section, we presented different mode dynamics of a push pull converter. Its model is well-known as switched model. In our project, we would like to design an indirect controller where we deal with average value of the control signal instead of modes. This average value, typically referred to as the duty cycle, will be central to our control approach.

Let us consider a switching period (see Fig. 2.2), the average model of the converter can be written in the following form:

$$\dot{X} = AX + B \tag{2.24}$$

where X is the average value of x over a switching period, U corresponds to the duty cycle D (see Fig.2.2). The state and input matrices are given by:

$$A = A_1 D + A_2(0.5 - D) + A_1 D + A_2(0.5 - D) = A_2 = A_1 \tag{2.25}$$

$$B = B_1 D + B_2(0.5 - D) + B_1 D + B_2(0.5 - D) = 2B_1 D \tag{2.26}$$

Thus, the above model becomes:

The Average mode of a push pull converter is given by:

$$\dot{X} = \mathbf{A}X + \mathbf{B}U \tag{2.27}$$

where $\mathbf{A} = A_1 = \begin{bmatrix} 0 & -\frac{1}{L} \\ \frac{1}{C} & -\frac{1}{RC} \end{bmatrix}$, $\mathbf{B} = 2B_1 = \begin{bmatrix} \frac{2Vg}{nL} \\ 0 \end{bmatrix}$, *and* $U = D$.

This model will be used in the next section for control design

2.4 Control design

Control systems are aimed to modify the behavior of an existing system to perform in a desired way. Several examples can be found in the real life in which certain control actions are needed to achieve the wanted results.

Control objective

In our context, we would like to regulate the output voltage of the push pull converter Vo around V_{ref}despite load and input voltage variations.

Several control techniques have been proposed in literature for controlling power converters. To mention a few, these include PID controllers, predictive and optimal control, fuzzy logic, and sliding mode control. In our master's project, we consider a linear quadratic regulator that will be applied on an augmented version of our system.

2.4.1 LQR Description

Linear quadratic regulator (LQR) is a closed-loop optimal control system that is used to minimize a quadratic cost function of the system's state and control variables. LQR is a popular choice for feedback control of linear systems.[7]

Consider the following state-space model:

$$\dot{x} = Ax + Bu \tag{2.28}$$

where A and B are matrices with constant time-invariant elements. The LQR problem provides a full state feedback law ($u = Kx$) that minimises

$$J = \frac{1}{2}\int_0^\infty [x^T Q x + u^T R u]dt \tag{2.29}$$

where Q and R are the state and control weighting matrices. The optimal gain K is given by:

$$K = -R^{-1}B^T\overline{P} \tag{2.30}$$

where $\overline{P}$ is an n$\times$ n positive definite, symmetric matrix. It corresponds to the solution of the nonlinear, matrix, algebraic Riccati equation (ARE):

$$\overline{P}A + A^T\overline{P} + Q - \overline{P}BR^{-1}B^T\overline{P} = 0 \tag{2.31}$$

2.4.2 LQR design for Push Pull Converter

To guarantee the output voltage follows its reference with steady state error, we consider the following integral term [8]:

$$\xi = \int (V_{ref} - V_o)dt \tag{2.32}$$

where V_{ref} is the set point (desired value of the output). By taking the first derivative of 2.4.2, we obtain

$$\dot{\xi} = V_{ref} - V_o \tag{2.33}$$

Now,ξ is an additional state to the push pull converter model given by eq (2.28). By combining the state-space model (2.28) and 2.33, we obtain

$$\begin{aligned} \dot{X} &= \mathbf{A}X + \mathbf{B}U \\ \dot{\xi} &= V_{ref} - \mathbf{C}X \end{aligned} \tag{2.34}$$

where C = [0 1] is the output matrix. We can write 2.34 compactly

$$\begin{bmatrix} \dot{x} \\ \dot{\xi} \end{bmatrix} = \underbrace{\begin{bmatrix} \mathbf{A} & 0 \\ -\mathbf{C} & 0 \end{bmatrix}}_{A_{aug}} \begin{bmatrix} x \\ \xi \end{bmatrix} + \underbrace{\begin{bmatrix} \mathbf{B} \\ 0 \end{bmatrix}}_{B_{aug}} u + \begin{bmatrix} 0 \\ 1 \end{bmatrix} V_{ref} \tag{2.35}$$

$$A_{aug} = \begin{bmatrix} 0 & -\frac{1}{L} & 0 \\ \frac{1}{C} & -\frac{1}{RC} & 0 \\ 0 & -1 & 0 \end{bmatrix}$$

$$B_{aug} = \begin{bmatrix} \frac{2Vg}{nL} \\ 0 \\ 0 \end{bmatrix}$$

The state-feedback controller now has the following form:

$$u = -\begin{bmatrix} K_x & K_\xi \end{bmatrix} \begin{bmatrix} x \\ \xi \end{bmatrix} = -K_x x - K_\xi \int (V_{ref} - V_o)dt$$

It should be noted that the performance index is given by:

$$J = \frac{1}{2}\int_0^\infty [x^T \ \xi] Q [x^T \ \xi]^T + u^T R u \ dt \tag{2.36}$$

where Q is a 3 × 3 matrix and R is 1 × 1 matrix. The LQR design involves solving the Algebraic Riccati Equation (ARE):

$$PA_{aug} + A_{aug}^T P + Q - PB_{aug}R^{-1}B_{aug}^T P = 0 \tag{2.37}$$

which can be challenging due to its reliance on matrix operations. Fortunately, MATLAB provides a straightforward solution to the LQR problem through the "lqr" command. Once the matrices Q, R, Aaug, and Baug are chosen, the feedback gain K can be easily calculated.

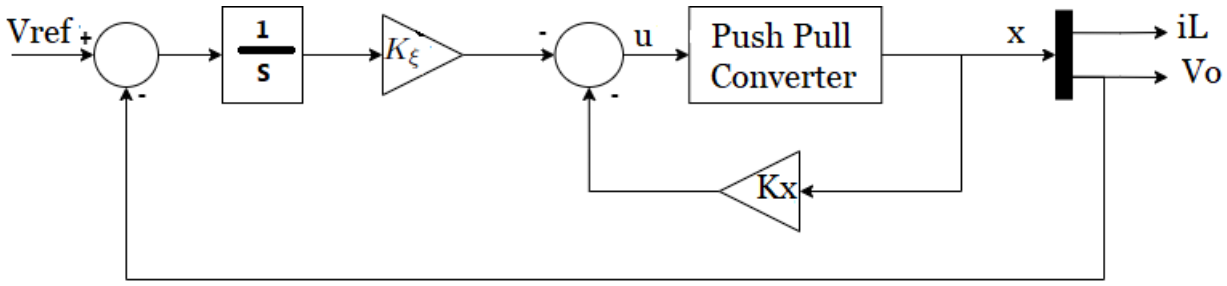

Figure 2.6: Representation of input–output linearization principle

2.5 Conclusion

In conclusion, this chapter has provided a comprehensive exploration of the operational principles of the push-pull converter, offering an in-depth analysis of its mathematical foundations. Furthermore, we have introduced a linear quadratic regulator designed specifically for the pushpull converter, with the primary goal of effectively regulating its output voltage.

Chapter 3

Experimental Setup

Contents

3.1 Introduction

This chapter presents the experimental workbench used for the verification and correctness of the control technique developed in the previous chapter. The Power converter design, construction, control and all experimental tests are conducted in LACoSERE laboratory at Laghouat University. Fig.3.1 shows the main parts of the test bench. The description of each element will be presented in detail in the following subsections.

3.2 Description of the test bench

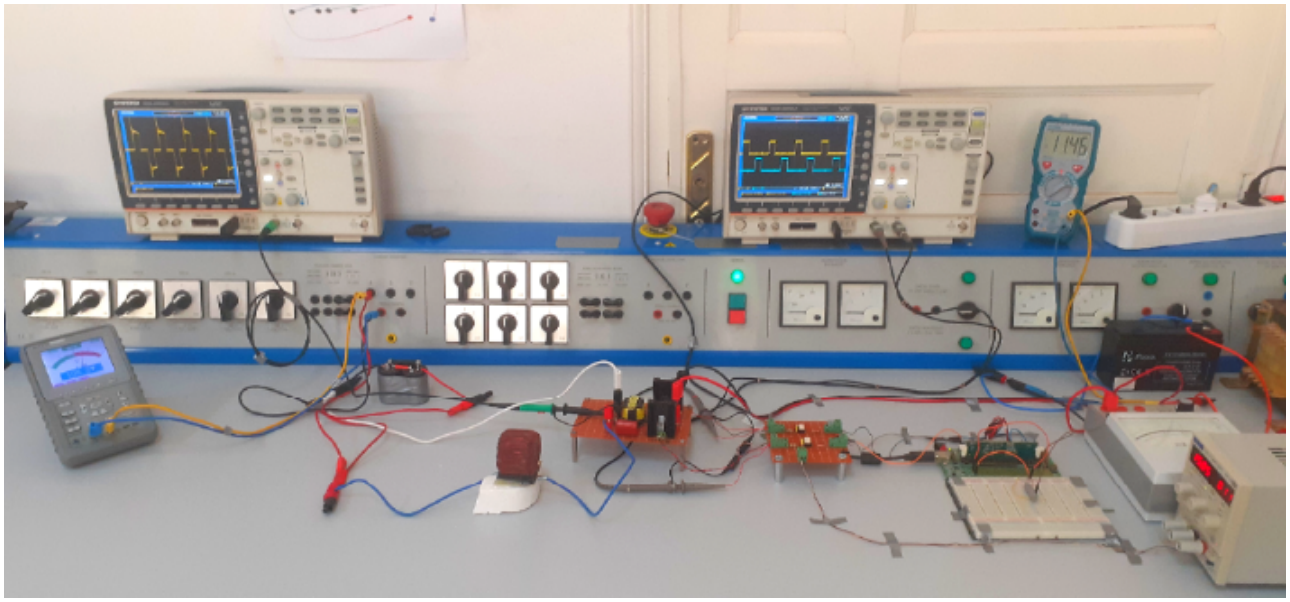

Figure 3.1: Experimental setup of push-pull converter.

In this section, we will present the test bench and the main hardware used in the validation process. As illustrated in Fig. 3.2, this test bench consists of:

- Push-pull converter,
- dSPACE 1103 board,
- DSP 28335 Experimenter Board,
- PWM signals isolation,
- current and voltage sensors,
- Oscilloscopes,
- Isolated DC power supplies,

- Inductor and resistive load.

  In the next sections, we will present each part with more details

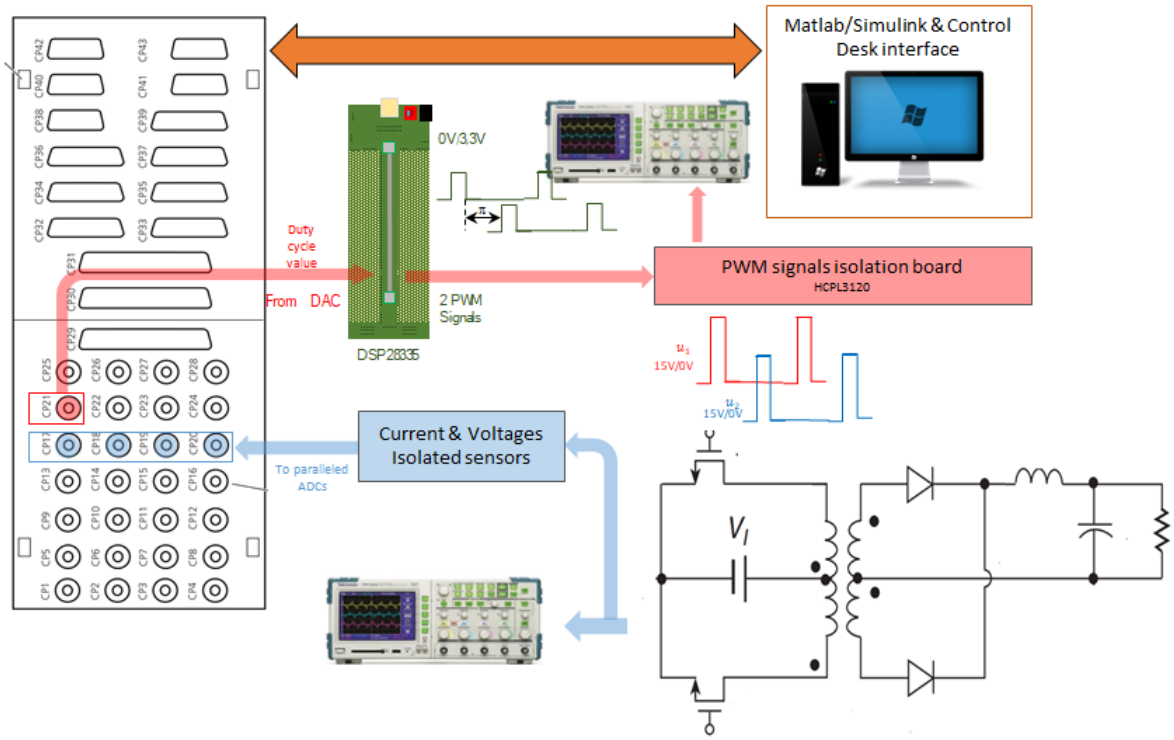

Figure 3.2: Schematic of the test bench

3.3 dSPACE Board

The DS1103 Fig 3.3 is an all-rounder in rapid control prototyping. Its processing power and fast I/O are vital for applications that involve numerous actuators and sensors. Used with Real-Time Interface (RTI), the controller board is fully programmable from the Simulink® block diagram environment. You can configure all I/O graphically by dragging RTI blocks. This is a quick and easy way to implement your control functions on the board[9].

The controller board is designed to meet the requirements of modern rapid control prototyping and is highly suitable for applications such as induction motor control, robotics, positioning systems and stepper motors, active vibration control, and rapid control prototyping for automotive controllers. In our experimental tests, the DS 1103 shown in Fig. 3.3 is used for:

- Measuring all the required signals, the inductor current of the push pull converter, the voltages of the output capacitor and of the input source, which is achieved using parallel channels of the A/D converter.

- Displaying and storing, when needed, in real time the measured signals by means of the Control Desk software interface.

Figure 3.3: dSPACE board.

- Performing the control law by generating duty cycle value, in real time, via the DACs connectors. The DACs (Digital to Analog Converters) can output voltages in the range of ±10volts. As the analog outputs are intended to be used as inputs in the DSP board, the output voltages are limited in Simulink, in order to generate voltages in the range of 0 to 3.3V1.

3.4 TMDSDOCK28335 Experimenter kit board

The TMDSDOCK28335, shown in Fig.3.4, is a development board designed by Texas Instruments (TI). This board is primarily used for prototyping and developing applications with the TI C2000 Piccolo TMS320F2833x microcontroller series, which is part of TI's family of real-time control microcontrollers. Key features and components of the TMDSDOCK28335 development board typically include[10]:

- **Microcontroller:** The board features a socket or space for installing a TMS320F28335 microcontroller. This microcontroller is known for its capabilities in real-time control and digital signal processing (DSP) applications.

- **I/O Interfaces:** The board provides various interfaces and connectors, such as GPIO (General-Purpose Input/Output) pins, analog input/output pins, and communication ports for connecting peripherals and sensors.

- **Onboard Debugging:** Many development boards like the TMDSDOCK28335 include integrated debugging and programming capabilities, allowing developers to load and debug firmware easily.

- **Power Supply:** There's typically a power supply section to provide the necessary voltage and current to the microcontroller and other components on the board.

The TMDSDOCK28335, like other TI development boards, is a valuable tool for engineers and developers working on applications such as motor control, power electronics, and other realtime control systems. It simplifies the process of designing and testing software and hardware solutions for these types of applications.

Figure 3.4: DSP Board.

In our project, the board is used**to generate two PWM control signals of 20KHz frequency, shifted in phase by 180 degrees** from each other (see Fig. 3.6). The card receives the duty cycle value from the control algorithm implemented in the Dspace control board.

3.5 PWM-signals isolation Board

A PWM signal isolation board serves to electrically isolate PWM signals, maintaining a separation between the source (typically a microcontroller) and the destination (often a power electronics circuit). This isolation enhances safety, reduces noise and interference, and enables compatibility between different voltage levels.

It ensures accurate and reliable transmission of control information, crucial in industrial applications such as motor drives, power inverters, and feedback systems, where precise control of high-power equipment is essential. In summary, PWM signal isolation boards are vital for maintaining the integrity, safety, and functionality of control signals in environments where electrical isolation is paramount.

Fig. 3.5 shows the developed isolation board which is used to:

1) isolate DSP PWM signals from the power stage,

2) increase the voltage level from $0 - 3.3V$ to $(0/ + 15V)$. The isolation has been achieved by the optocoupler HCPL-3120 (one for each signal). The HCPL-3120 consists of an infrared

light-emitting diode (LED) and a photodetector integrated into asingle package.

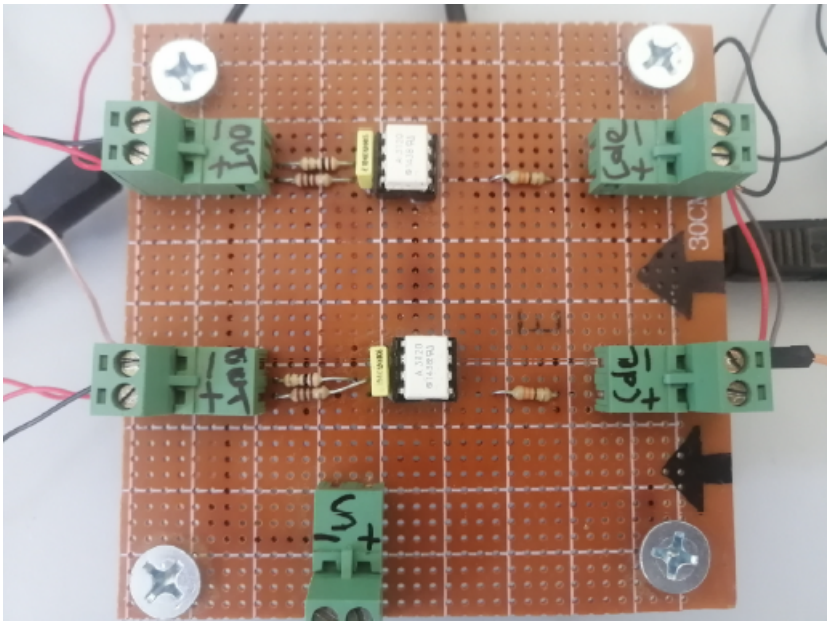

Figure 3.5: PWM-signals isolation board.

Fig.3.6 shows an example of the output of this card which consists of two isolated PWM signals with 25% duty cycle, shifted by 180 degrees, and 20KHz frequency.

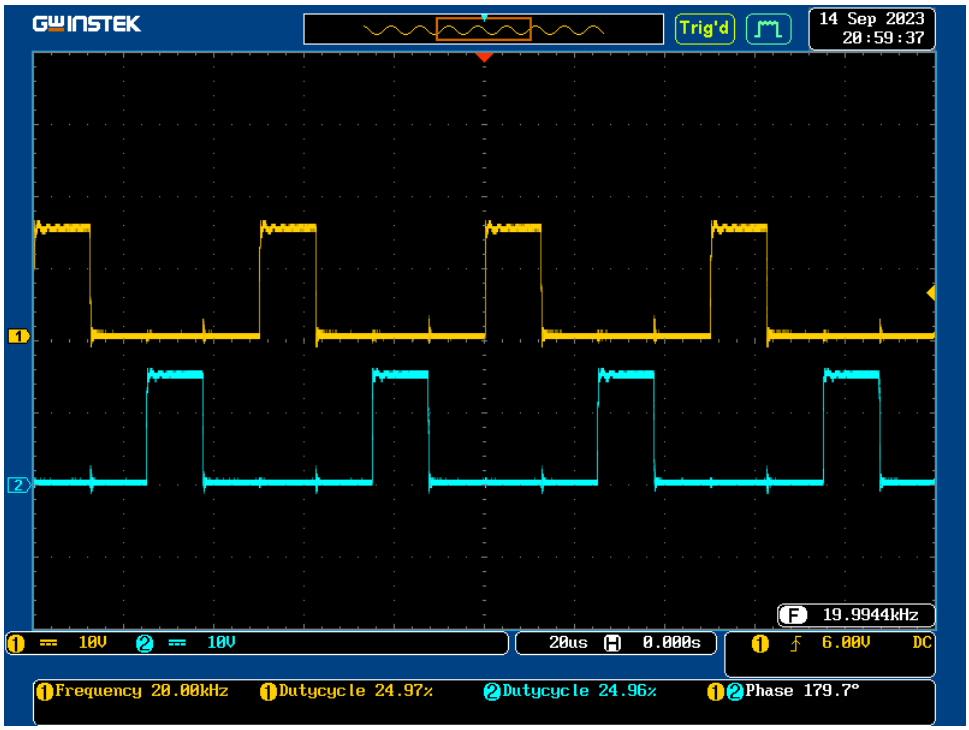

Figure 3.6: PWM shifted signals generated by the isolation Board (0v/15v).

3.6 Push-pull converter

The implemented push-pull converter is shown in Fig 3.7 which consists of the following elements:

- Two power MOSFETs (IRFP260M),
- A pulse transformer recycled from a defective solar inverter,
- Quadrature rectifier and two capacitors, connected in parallel at the input of the transformer,
- and an external L-C filter connected at the output of the transformer.

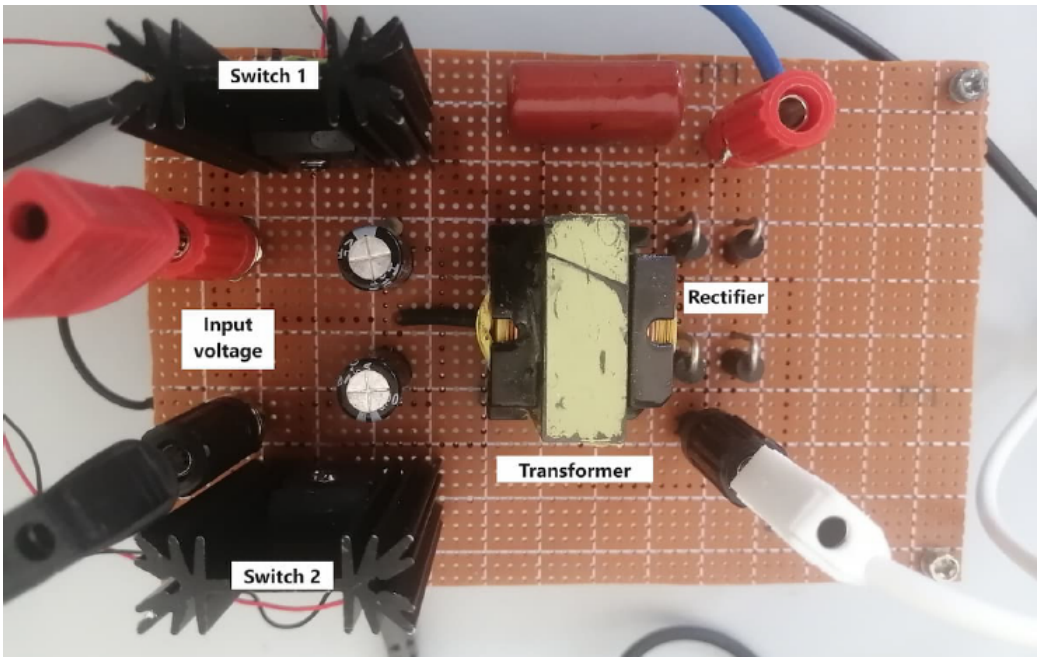

Figure 3.7: The developed Push-Pull Converter

3.7 Voltage and current Sensors

In order to ensure an isolation between the power stage and the control unit, we used for the measurements isolated voltage sensors that use optically isolated amplifiers designed specifically for voltage sensing, and Hall-effect based current sensors, which are galvanically isolated sensors. Fig. 3.8 shows the sensors used in the experimental tests.

At this level, we presented an overview about the developed experimental setup and the next chapter will be devoted to testing the converter operation under the proposed control law.

Figure 3.8: Current and voltage measurement sensors

3.8 Conclusions

In this chapter, we discussed different parts of the experimental setup which correspond to the converter and its auxiliary boards, the dSPACE and DSP control boards, and measurement devices. The control scheme developed in the second chapter will be implemented in the dSPACE board using Matlab/Simulink to test its effectiveness. This is the aim of the next chapter.

Chapter 4

Simulations&Experimental Results

Contents

4.1 Introduction

This chapter presents the main results obtained from simulations and experimental setup of the push pull converter. We initially examine its performance in an open-loop configuration, followed by an assessment of the effectiveness of the linear quadratic regulator in controlling the push-pull converter when operating in a closed-loop configuration.

4.2 Simulation results

The push-pull converter has been implemented within Simulink/Matlab, utilizing electrical components from the Simscape package. Consequently, the model employed for the converter differs from the ideal one described in Chapter 2, aligning more closely with a realistic representation.

Fig. 4.1 illustrates the integrated closed-loop system in Simulink/Matlab, encompassing both the converter and the controller. The control scheme, referred to as the PI controller in Fig. 4.1, is presented in Fig. 4.2.

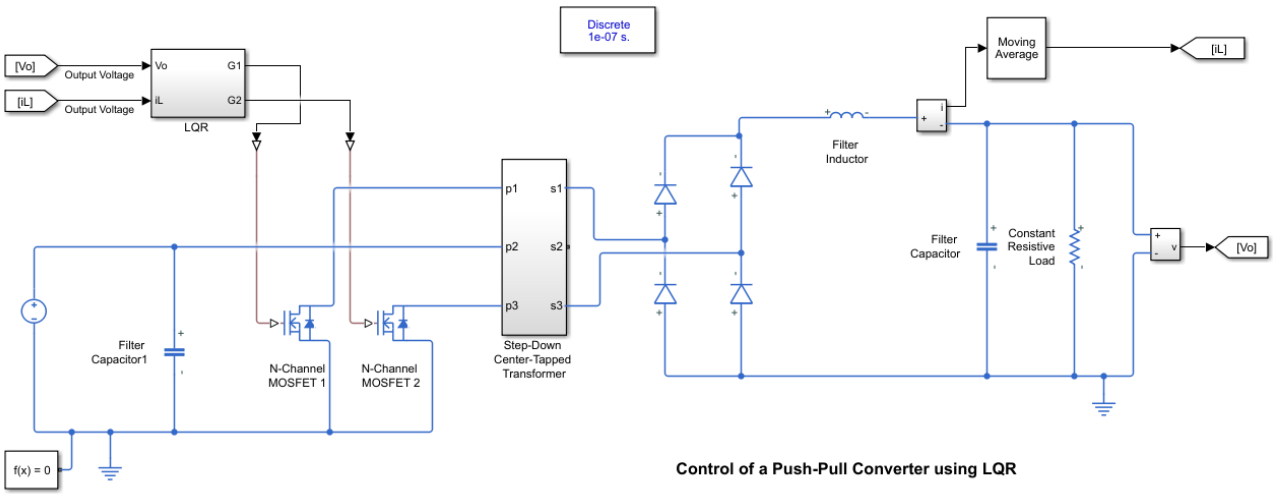

Figure 4.1: Controlled Push-pull converter scheme in Simulink/Matlab.

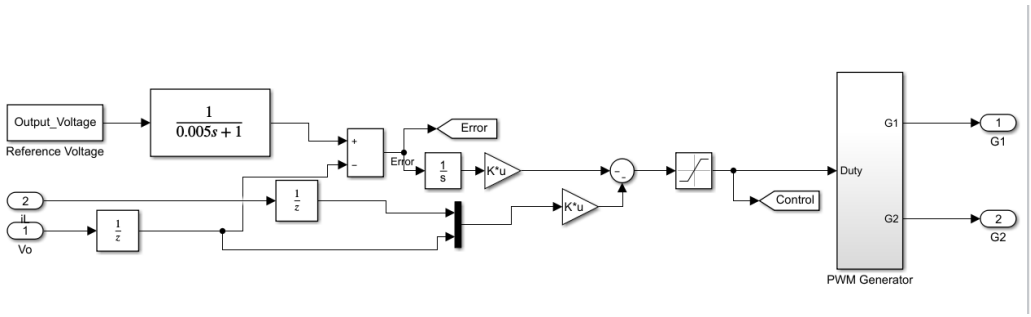

Figure 4.2: Linear quadratic regulator and PWM generator

The implemented push-pull converter shares parameters that closely resemble those of the experimental setup:

- Input voltage Vg = 12V
- Output filter: $L = 1.57mH$, C = 340μF
- Resistive load R = 217Ω
- The ratio of voltage transformation of a transformer is 16.
- PWM generator frequency f = 20kHz.

4.2.1 Open loop simulations of push-pull converter

In this subsection, we set the duty cycle to 0.499 to have an idea about the maximum voltage that the push pull converter can provide for an input voltage with Vg = 12V. The following figure shows the

obtained result where the output voltage reach a maximum of 375V. This is less than the expected value:

$$Vo = 2 * 2 * DVg/n = 2 * 2 * 0.499 * 12 * 16 = 383.23V$$

This mainly returns to the transformer and rectifier voltage losses.

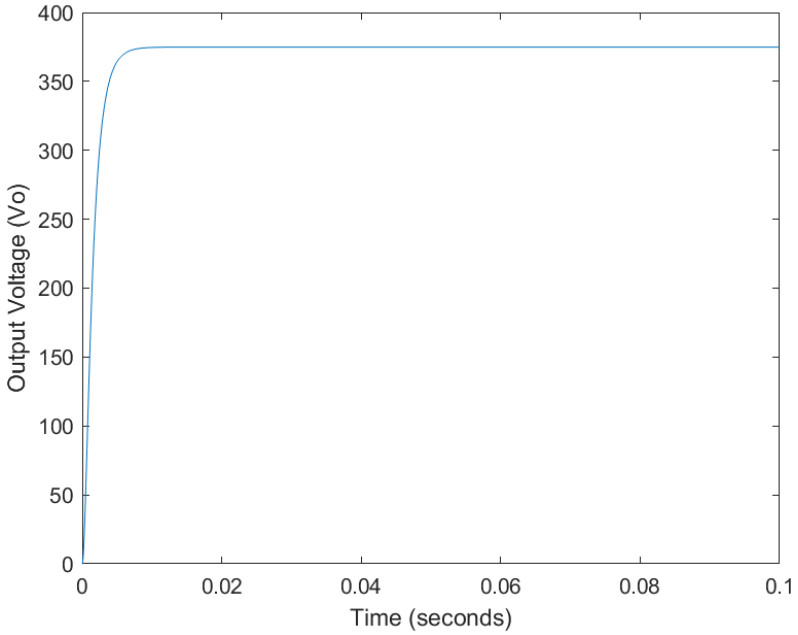

Figure 4.3: The output voltage of a push pull Converter for a duty cycle close to 50%.

4.2.2 Closed loop simulations of push-pull converter

The state feedback gain K is obtained by solving the Riccati equation (see Chapter 2) for our system with the parameters provided above. The weight matrices (state and input matrices) of the performance index are chosen as follows:

$$Q = \begin{bmatrix} L & 0 & 0 \\ 0 & C & 0 \\ 0 & 0 & 1e^7 \end{bmatrix}, R = 1$$

The above elements of the matrix Q are chosen with respect to the stored energy in each element of the filter LC. The weight value of the integral term (ξ) is chosen by trial and error.

It should be noted that we used Matlab to solve the algebraic Riccati equation. This can be achieved by the following syntax:

$$[K, S, P] = lqr(A, B, Q, R)$$

where K the optimal gain matrix, S is the solution of the associated algebraic Riccati equation (denoted $\overline{P}$ in Chapter 2) , and P is the closed-loop poles.

The obtained state feedback gain of the augmented system is given by:

$$\mathrm{K} = [0.0855 \quad 0.239 \quad -10^3 \,]$$

Scenario 1: Variable reference voltage

During this simulated experiment, we varied the reference voltage every 0.2 seconds, cycling through values of 50V, 60V, and 80V. Fig. 4.4 shows the output voltage and its reference. The controller effectively achieved rapid response (within 35 milliseconds), ensuring that the output voltage closely followed its reference with zero steady state error.

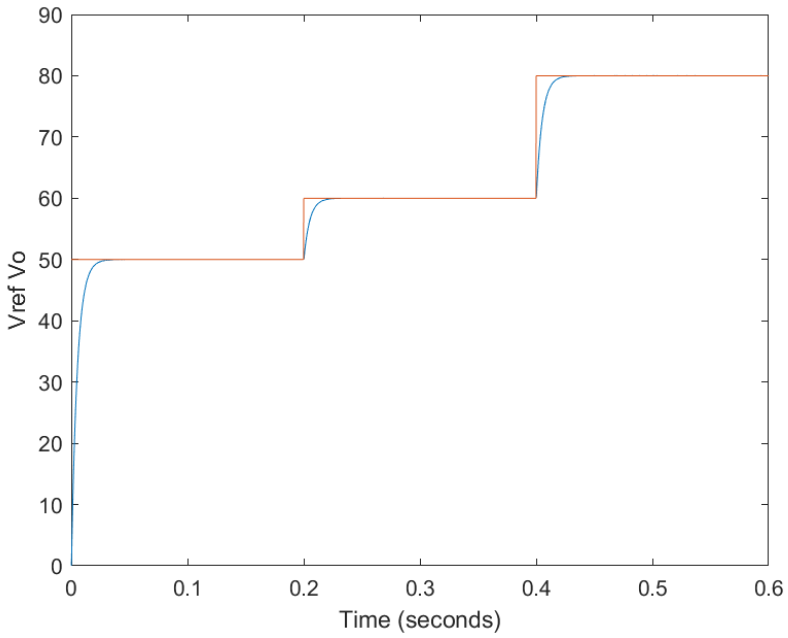

Figure 4.4: The voltage of the Converter with change in reference voltage

By modifying the weight matrices Q and R, the response time of the closed-loop system can be customized to meet specific requirements.

Scenario 2: Variable load

In order to assess the controller's robustness against load fluctuations, we established a reference voltage of 100V while varying the resistive load from 217 to 108.5 at 0.05s. The obtained results, depicted in Fig. 4.5 and Fig. 4.6, demonstrate the controller's effectiveness in promptly mitigating load changes and ensuring accurate tracking of the reference voltage.

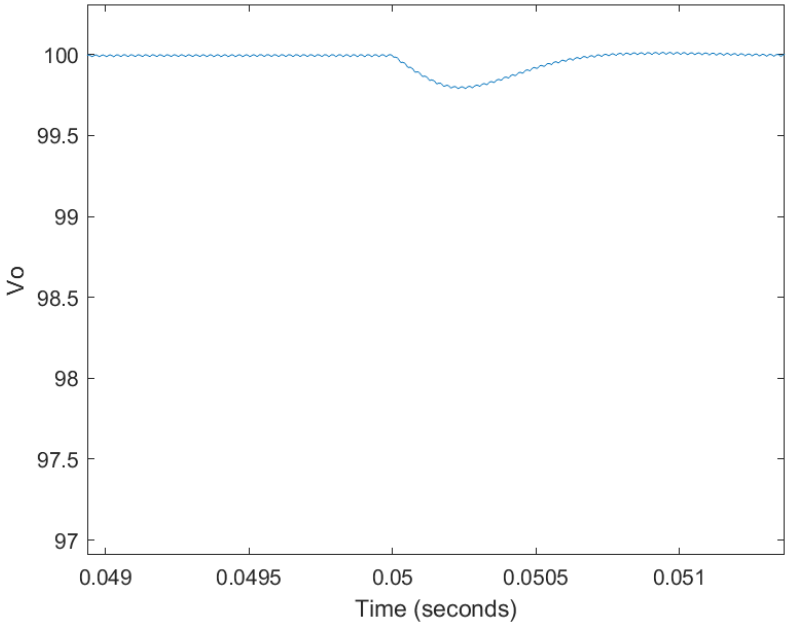

Figure 4.5: The output voltage of the converter under a sudden change of the load.

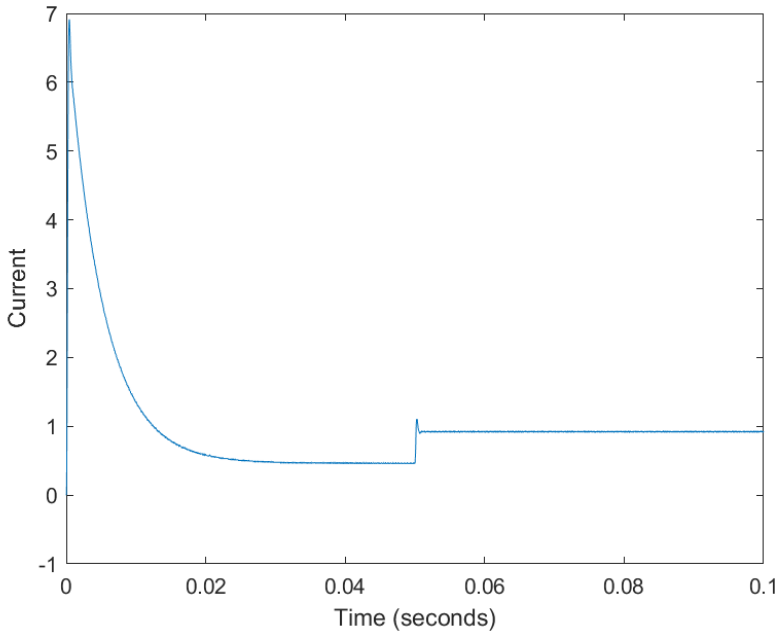

Figure 4.6: The output current of the converter under a sudden change of the load.

Scenario 3: Variable input voltage

In this particular scenario, we established a reference voltage of 100V and maintained a load resistor of 217Ω. At t=0.05s, we introduced an initial change in the input voltage Vg, reducing it from 12V to 11.5V. Subsequently, at t=0.1s, we initiated another variation, lowering the input voltage further to 10V.

Fig. 4.7 displays the results obtained in this scenario, clearly illustrating that the closed-loop

system exhibits insensitivity to fluctuations in the input voltage.

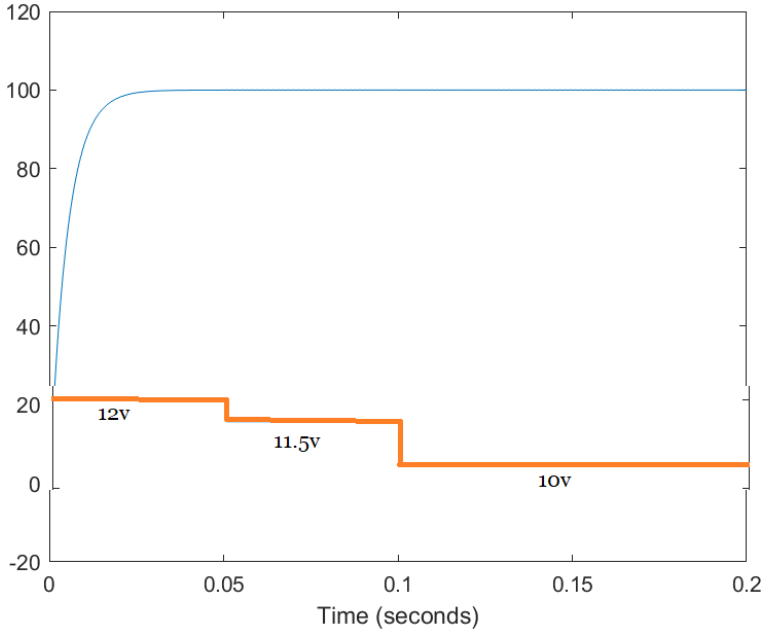

Figure 4.7: The voltage of the push pull converter under input voltage variations.

In summary, the suggested controller has demonstrated effectiveness in maintaining the output voltage close to its reference value, even in the presence of load and input voltage fluctuations. In the subsequent section, we will conduct similar tests using the experimental setup.

4.3 Experimental results

The control law is implemented in Simulink/Matlab together with RTI (real time interface) blocks of the dSPACE for measurement and duty cycle generation. The sampling time is set to 10s and measured signals are processed with first-order lowpass filter with time constant 1ms.The dSPACE board sends average value of control signal (duty cycle) to the DSP. The latter generates two shifted PWM signals as explained in the previous chapter. The system parameters, encompassing input voltage, load resistance, LC filter, and switching frequency, remain consistent with those employed in the simulation phase.

4.3.1 Open-loop control: experimental results

Fig. 4.8 illustrates the open loop scheme implemented in Matlab/Simulink with RTI blocks and loaded to the dSPACE for real time tests. We used three ADC (analog to digital converter) of the dSPACE to acquire the input voltage, output voltage and inductor current. We used one DAC (digital to analog

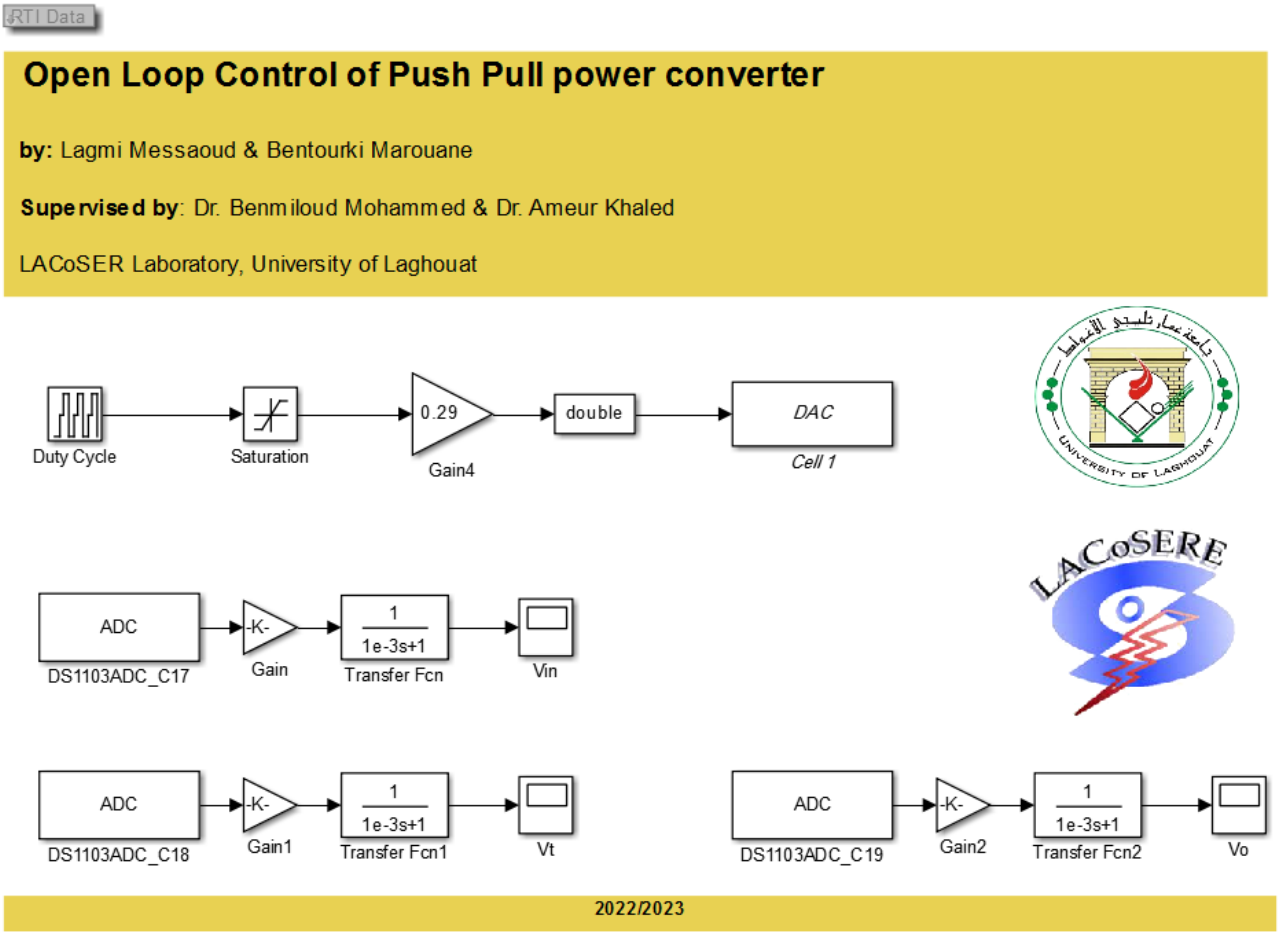

Figure 4.8: Open loop control implementation in Simulink/Matlab & RTI blocks

converter) to send the duty cycle to the DSP board. In this particular scenario, the duty cycle follows a recurring sequence with 1-second intervals,oscillating between values of 0.15, 0.2, and 0.25 (see Fig. 4.9).

Fig. 4.10 illustrates the voltage at the output of the transformer in steady state for different duty cycle values (0.15, 0.2, 0.25). It has three voltage levels as explained in Chapter 2, 2DVg/n, 0, and 2DVg/n.

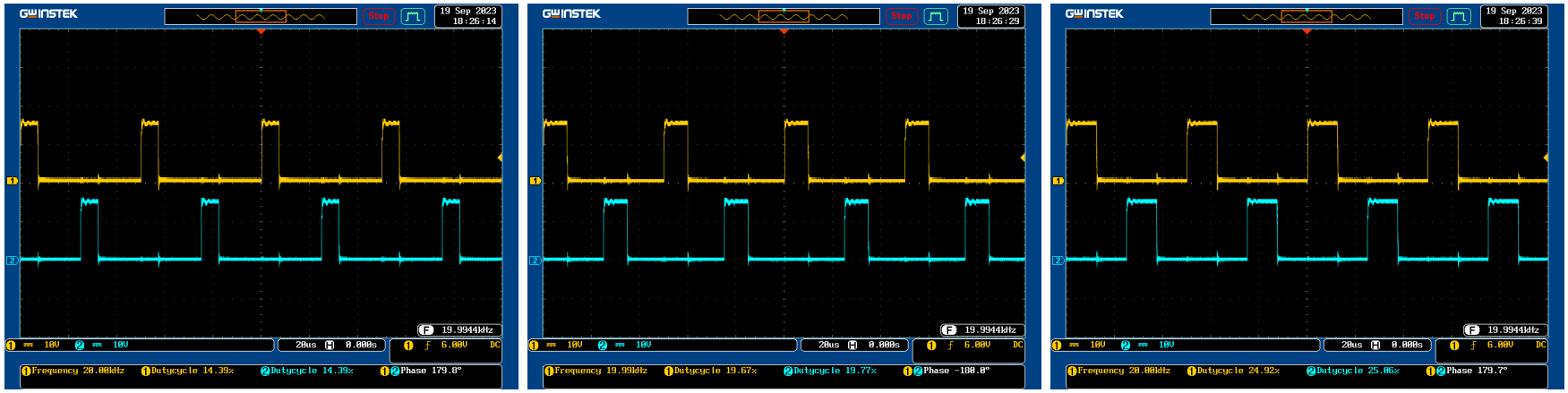

(a) (b) (c)

Figure 4.9: The control signals at the output of the isolation board in steady state for different duty cycle values (0.15, 0.2, 0.25).

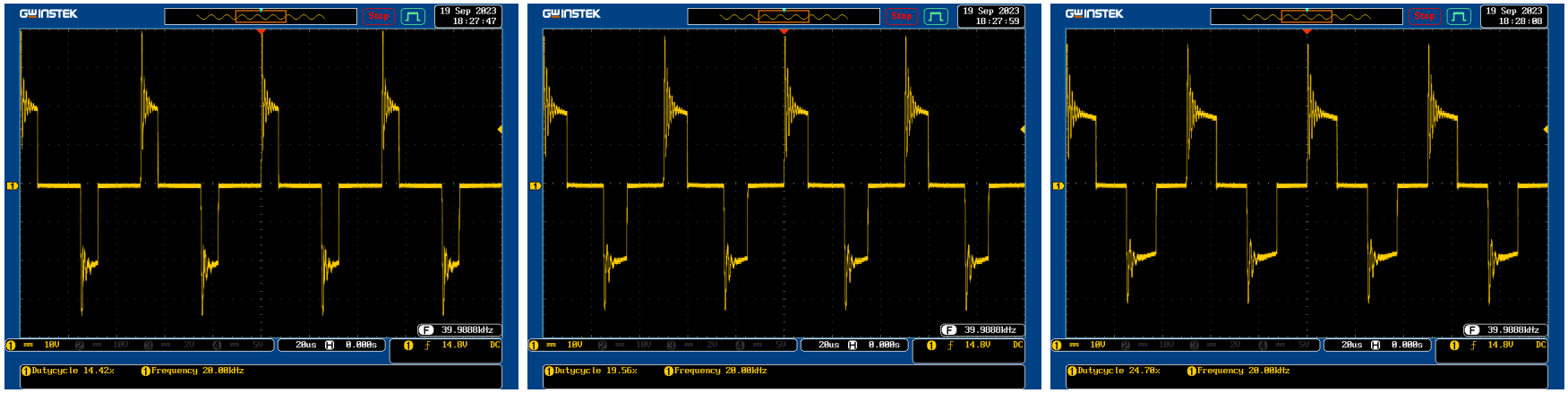

(a) (b) (c)

Figure 4.10: The voltage at the output of the transformer in steady state for different duty cycle values (0.15, 0.2, 0.25).

Fig.4.11 shows the output voltage of the push pull converter under the repeating sequence of the duty cycle. It should be noted that for safety reasons, we didn't take high values for the duty cycle.

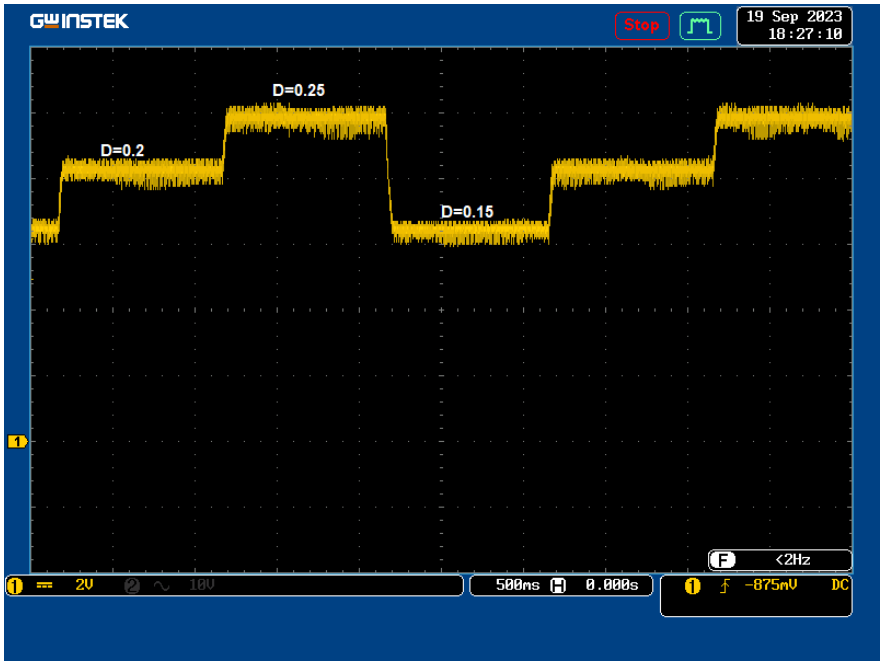

Figure 4.11: The output voltage of the push pull converter in open loop.

4.3.2 Closed-loop control: experimental results

Fig.4.12 illustrates the implemented LQR in Simulink/Matlab with RTI blocks In experimental tests, we have changed the third element of the state feedback gain from -10^3 to -10 (stability of the closed loop system is verified). This returns to the saturation of the control signals.

Scenario 1: Variable reference voltage

In this scenario, we varied the reference voltage every 1 second, cycling through values of 50V,60V, and 80V. This corresponds to the same test shown in Fig. 4.4. The obtained experimental results are given in Fig. 4.13. The input voltage (in yellow) is set to 12V by the mean of a DC power supply. The output voltage (in blue) follows its reference with zero steady state error, in average.

The control signal (duty cycle) in green exhibit a saturation when the reference voltage changes abruptly from 80V to 50V. In overall, the controller is efficient and guarantees fast response (less than 50ms).

Scenario 2: Variable load

In this experiment, we change the resistance between values (145Ω, 217Ω, 362Ω) and set the reference voltage to 60V. The result is shown in the fig 4.14, clearly illustrating that the controller effectively stabilizes the output voltage , despite the output resistance variations.

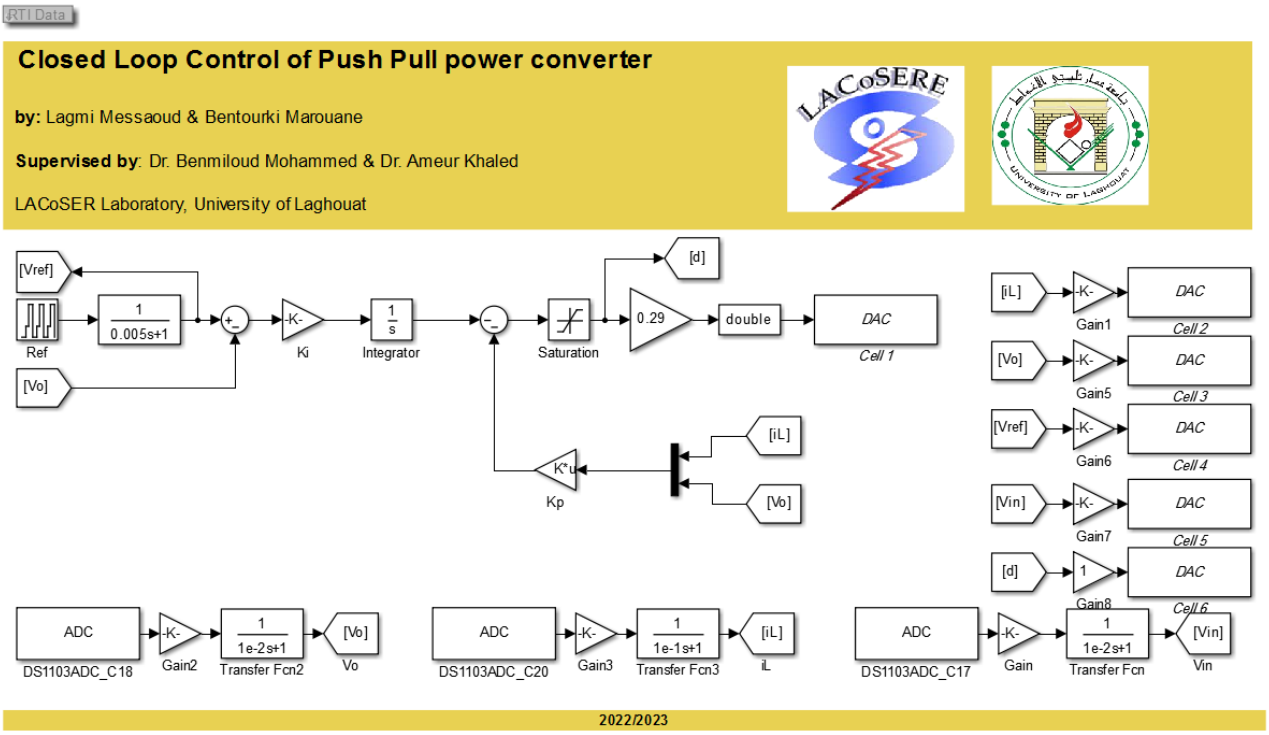

Figure 4.12: Closed loop control implementation in Simulink/Matlab RTI blocks

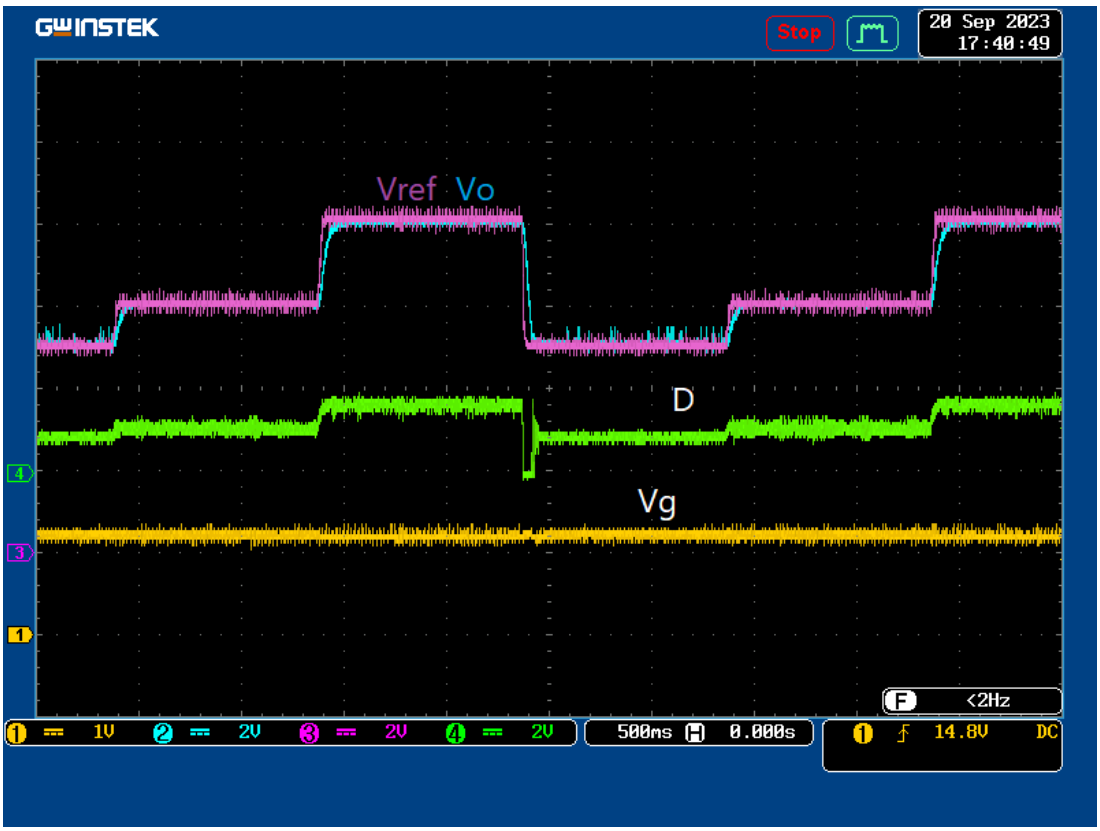

Figure 4.13: Top: Output voltage and reference voltage [Vo,Vref], Middle: Control value [D], Bottom: Input voltage [Vg]

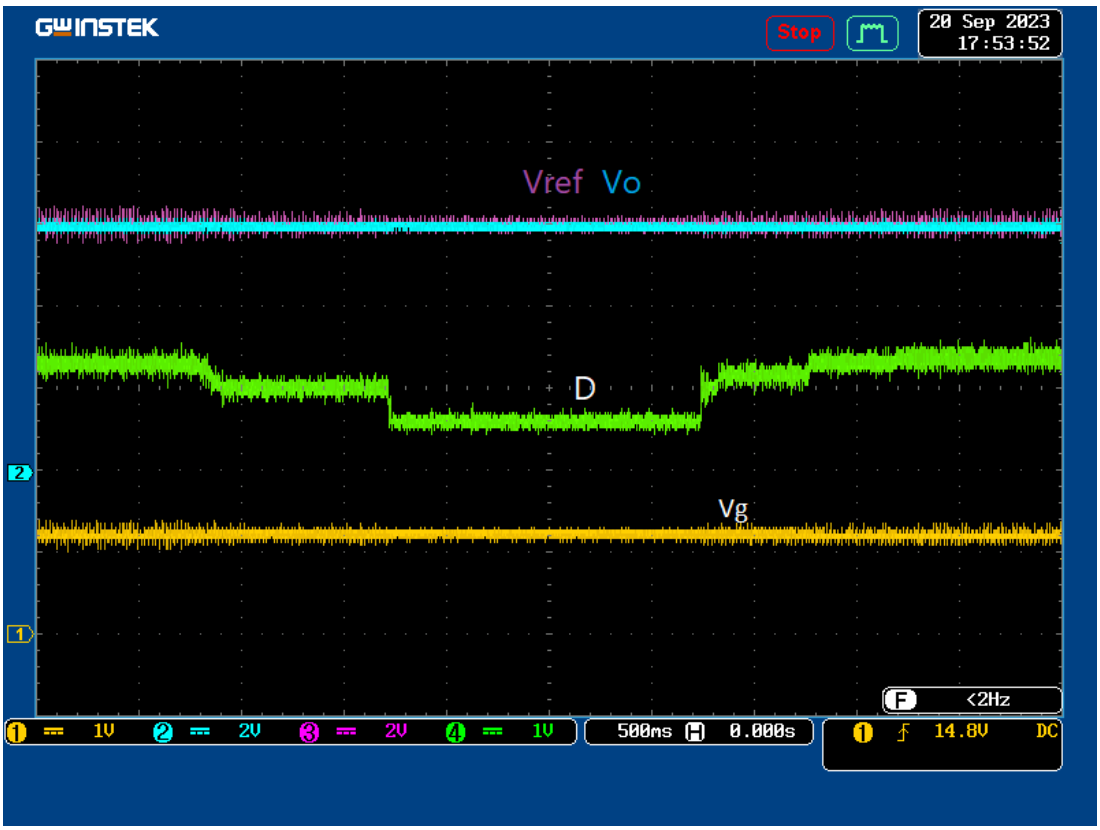

Figure 4.14: Top: Output voltage and reference voltage [Vo,Vref], Middle: Control value [D], Bottom: Input voltage [Vg]

Scenario 3: Variable input voltage

In this particular scenario, we established a reference voltage of 60V and maintained a load resistor of 217Ω. We perturbed the input voltage Vg around 12V. The obtained results are shown in Fig. 4.15. It is clear that the controller is able to achieve a good stabilization of the output voltage despite the input voltage variations. The input voltage variations were made manually using the laboratory DC power supply

To sum up, the proposed controller has undergone rigorous evaluation through a series of simulation and experimental tests, including three key scenarios:

- **Variable Reference Voltage Test:** In this test, the controller exhibited remarkable efficiency and demonstrated a fast response time, consistently achieving stabilization within 50 ms.
- **Variable Load Test:** The outcomes of this test proves the controller's ability to maintain stable output voltage even when faced with varying output resistance. Impressively, it proved to be highly insensitive to such disturbances.
- **Variable Input Voltage Test:** This test revealed the controller's exceptional capability to ensure stable output voltage in the presence of fluctuations in the input voltage.

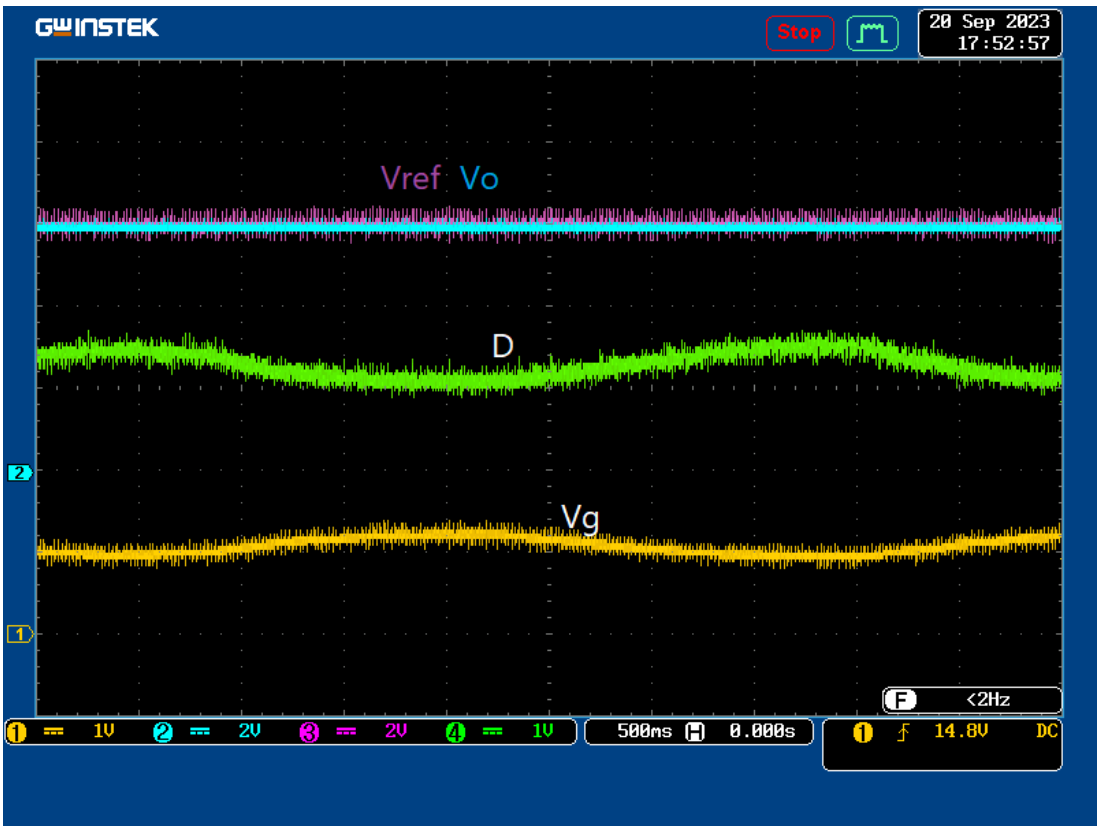

Figure 4.15: Top: Output voltage and reference voltage [Vo,Vref], Middle: Control value [D], Bottom: Input voltage [Vg]

4.4 Conclusions

In this chapter, we have presented different simulation and experimental results. In summary, the proposed controller has demonstrated consistent and impressive performance under a set of challenging scenarios.

General Conclusion

This project is part of the work carried out within the Automatic Complex Systems Team of the LACoSERE laboratory on the subject of static converters control used for photovoltaic systems. One of the objectives is to investigate new power conversion structures with advanced control strategies.

The work presented in this master thesis is devoted to the implementation and control of a push pull power converter, mainly used in solar inverters in the DC-to-DC stage. The project objectives have been successfully attained and comprehensively outlined within the four chapters:

In **Chapter One**, we introduced DC/DC power converters, emphasizing the distinction between Isolated and non-isolated topologies. Additionally, we presented an algorithm designed to guide the selection of the most suitable power converter topology for a given application based on power, voltage, and current specifications. At the end of the chapter, we explained our reasons for choosing the push-pull converter.

In **Chapter Two**, we discussed the operational principles of a push-pull converter in detail, exploring its mathematical foundations. Towards the chapter's conclusion, we introduced the average model of the converter, a key component in our controller design. The latter corresponds to a linear quadratic regulator, which has been applied to an augmented system (converter model and integral action).

In **chapter three**, we have explored various components of the experimental setup, encompassing the converter and its auxiliary boards, the dSPACE and DSP control boards, and measurement devices.

The last **chapter showcases** the primary outcomes derived from simulations and experimental trials involving the push-pull converter. We started by evaluating its performance in an openloop setup, followed by a comprehensive analysis of the effectiveness of the linear quadratic regulator in controlling the push-pull converter under load and input voltage variations.

The proposed controller has undergone rigorous evaluation in a series of simulation and experimental tests, including three key scenarios (reference voltage, load, and input voltage variations). In various demanding situations, the controller consistently demonstrated remarkable performance

As future work, we propose the following:

1 Implementing a solar inverter by integrating the push-pull converter into the DC-to-DC stage

and employing a single inverter in the DC-to-AC stage.

2 Evaluate the controlled push pull converter in practical environment with batteries and solar panels as an input voltage source.

3 Exploring direct control strategies based on the instantaneous model to enhance control and efficiency.

Bibliography

[1] Shafinaz A Lopa, Shahzad Hossain, MK Hasan, and TK Chakraborty. Design and simulation of dc-dc converters. International Research Journal of Engineering and Technology (IRJET), 3(01):63–70, 2016.

[2] Nakul Shah. Analysis, Design and Experimental Verification of a Novel AC-AC Buck Boost Based Dynamic Voltage Regulator. PhD thesis, The University of North Carolina at Charlotte, 2017.

[3] Sung-Jun Park, Jin Wook Park, Kuk Hyeon Kim, and Feel-Soon Kang. Battery energy storage system with interleaving structure of dual-active-bridge converter and non-isolated dc-to-dc converter with wide input and output voltage. IEEE Access, 10:127205–127224, 2022.

[4] Amin Emrani, Ehsan Adib, and Hosein Farzanehfard. Single-switch soft-switched isolated dc–dc converter. IEEE Transactions on Power Electronics, 27(4):1952–1957, 2011.

[5] F Dong Tan. The forward converter: From the classic to the contemporary. In APEC. Seventeenth Annual IEEE Applied Power Electronics Conference and Exposition (Cat. No. 02CH37335), volume 2, pages 857–863. IEEE, 2002.

[6] Yazdan H Tabrizi, M Nasir Uddin, and Hesamodin Allahyari. A high-gain bipolar pulse power generator employed bidirectional switch for dielectric barrier discharge applications based on resonance charging technique. In 2021 IEEE Industry Applications Society Annual Meeting (IAS), pages 1–7. IEEE, 2021.

[7] D Roy Choudhury. Modern control engineering. PHI Learning Pvt. Ltd., 2005.

[8] Heri Purnawan, Eko Budi Purwanto, et al. Design of linear quadratic regulator (lqr) control system for flight stability of lsu-05. In Journal of Physics: Conference Series, volume 890, page 012056. IOP Publishing, 2017.

[9] Derouich Aziz, Bouchnaif Jamal, Zamzoum Othmane, Mezioui Khalid, Badre Bossoufi, et al. Implementation and validation of backstepping control for pmsg wind turbine using dspace controller board. Energy Reports, 5:807–821, 2019.

[10] Eli Flaxer, Alona Flaxer, Moran Sapir, Lanna Bram, Yael Roichman, and Yuval Ebenstein. Portable low-cost and highly accurate programmable triggering controller for confocal spinning disk image scanning microscope. Ultramicroscopy, 249:113736, 2023.